Article

Formation of CoA Adducts of Short-Chain Fluorinated Carboxylates Catalyzed by Acyl-CoA Synthetase from *Gordonia* sp. Strain NB4-1Y

Robert G. Mothersole, Foster T. Wynne, Gaia Rota, Mina K. Mothersole, Jinxia Liu, and Jonathan D. Van Hamme*

Cite This: *ACS Omega* 2023, 8, 39437−39446

Read Online

ACCESS | Metrics & More | Article Recommendations | Supporting Information

ABSTRACT: Perfluoroalkyl and polyfluoroalkyl substances (PFAS) make up a group of anthropogenic chemicals with a myriad of applications. However, some PFAS have been shown to negatively impact human health and the environment, leading to increased regulation, with some countries making efforts to phase out their use. PFAS fate in the environment is driven by physical, chemical, and biological processes, with microbial communities in matrices such as soil and sewage sludge being known to generate a range of low-molecular-weight PFAS metabolites. Proposed metabolic intermediates for both mixed and pure microbial cultures include fluorinated carboxylates that may be activated by CoA prior to β-oxidation and defluorination, although thus far, no PFAS-CoA adducts have been reported. Herein, we expressed and purified acyl-CoA synthetase (ACS) from the soil bacterium *Gordonia* sp. strain NB4-1Y and performed an analysis of substrate scope and enzyme kinetics using fluorinated and nonfluorinated carboxylates. We

determined that ACS was able to catalyze the formation of CoA adducts of 3,3,3-trifluoropropionic acid, 5,5,5-trifluoropentanoic acid, 4,5,5-trifluoropent-4-enoic acid, and 4,4,5,5,5-pentafluoropentanoic acid. Kinetic analysis revealed a 90−98% decrease in k_{cat} between nonfluorinated carboxylates and their fluorinated analogues. This provides evidence to validate proposed enzymatic pathways for microbial PFAS metabolism that proceed via an activation step involving the formation of CoA adducts.
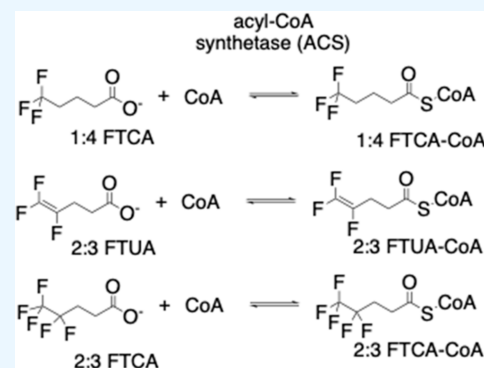
INTRODUCTION

Perfluoroalkyl and polyfluoroalkyl substances (PFAS) are a group of xenobiotics that are of concern due to their toxicity to humans and animals.[1−3] PFAS are widespread, persistent pollutants due to their resistance to degradation and participation in long-range environmental transport.[4−7] PFAS have made headlines as the level of these chemicals found in drinking water around the world has been determined to be higher than projected.[8] Between 0.4 and 1 million people in the United States are served drinking water contaminated with PFAS in excess of the Environmental Protection Agency's drinking water health advisory of 70 ng/L.[9] Some studies have suggested that this level is too high, and the safe limit should be as low as 1 ng/L, which would impact 50−80% of the US population.[10]

One major use of PFAS has been in aqueous film-forming foams (AFFFs), used primarily to combat hydrocarbon fuel fires at airports and on ships.[11] Some AFFFs contain high levels of 6:2 fluorotelomer sulfonamidoalkyl betaine (6:2 FTAB) and 6:2 fluorotelomer sulfonate (6:2 FTSA), compounds that have been detected in soil and groundwater at firefighting training centers.[12] At a decommissioned firefighting training center in western Canada where AFFF was routinely used, it was found that bacteria from the genus

Gordonia were found in abundance in the soil,[13] suggesting that this organism might be able to metabolize the PFAS there.

Indeed, while not from this site, the aerobic soil bacterium, *Gordonia* sp. strain NB4-1Y, was observed to utilize 6:2 FTAB and 6:2 FTSA as sources of sulfur for growth, generating 16 observable metabolites over a 7-day incubation.[14,15] Metabolites included a series of saturated (FTCA) and unsaturated (FTUA) fluorotelomer carboxylate intermediates. Intermediates such as 5:3 FTCA, perfluorobutanoic acid, perfluoropentanoic acid, perfluorohexanoic acid, and perfluoroheptanoic acid have also been observed in other pure bacterial cultures, enrichment cultures, at contaminated sites, and in sewage treatment plants.[16−18]

Nonfluorinated acyl-carboxylates can be metabolized by both eukaryotic and prokaryotic organisms via a β-oxidation pathway. This pathway is made up of an activation step where an acyl-CoA adduct is formed followed by four main steps.[19] First, acyl-CoA undergoes dehydrogenation catalyzed by acyl-

CoA-dehydrogenase to yield *trans*-Δ^2-enoyl-CoA. Then, there is hydration of the double bond via enoyl-CoA hydratase to form L-β-hydroxyacyl CoA. The third step is oxidation catalyzed by 3-hydroxyacyl-CoA dehydrogenase resulting in β-ketoacyl CoA. Finally, there is thiolysis by β-ketothiolase to produce an acyl-CoA shortened by two carbon atoms and acetyl-CoA. It has been proposed that fluorinated acyl-carboxylates such as 8:2 FTCA, 6:2 FTCA, and 8:2 FTUA may be metabolized via this process in microbial cultures.[15,20,21] However, there is some debate over whether these PFAS can be metabolized via this β-oxidation pathway due to an absence of hydrogens on the β-carbon.[22,23] In addition, to date, identification of PFAS-CoA adducts in microbial cultures has yet to have been reported, and the formation of acyl-CoA adducts is required prior to any β-oxidation pathway.[24]

A study by Che et al. (2021) found that microbial communities in activated sludge could metabolize short chain PFAS such as 3,3,3-trifluoropropionic acid (1:2 FTCA), 4,5,5-trifluoropent-4-enoic acid (2:3 FTUA), and 5,5,5-trifluoropentanoic acid (1:4 FTCA) and proposed the formation of a CoA adduct as the first step in metabolism.[25] While transcriptomic analysis with these substrates has not been performed on *Gordonia* sp. strain NB4-1Y, it is plausible that the bacterium may contain metabolic pathways similar to those found in the activated sludge studied by Che et al. (2021).

In prokaryotes, the biosynthesis of CoA adducts of short-chain fatty acids is catalyzed ([Figure 1](#)) by acyl-CoA
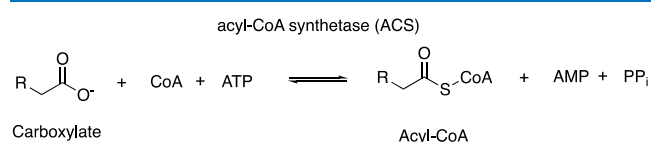
Figure 1. Scheme showing the reaction catalyzed by acyl-CoA synthetase.

synthetases (also referred to as acyl-CoA ligase).[26] Acyl-CoA synthetase, alongside nonribosomal peptide synthetase adenylation domains, and luciferases (ANL) make up a superfamily of adenylating enzymes.[27] Proteins in the ANL superfamily have some structural similarity, with 10 conserved binding motifs (A1–A10), but differ in their catalytic mechanism.[28] Acyl-CoA synthetase proceeds via a two-step ping-pong mechanism.[29] The first step involves adenosine triphosphate (ATP) binding, resulting in the formation of an acyl-adenylate enzyme bound intermediate, while the second step releases acyl-CoA and adenosine monophosphate (AMP). In eukaryotic organisms there are commonly multiple acyl-CoA synthetases that are specific to the activation of either short-chain (EC 6.2.1.1), medium-chain (EC 6.2.1.2), or long-chain fatty acids (EC 6.2.1.3).[30] Prokaryotic organisms, such as *Escherichia coli*, have fewer variations of acyl-CoA synthetase; consequently, those enzymes tend to have a broader substrate scope.[26]

Genomic and proteomic characterization of *Gordonia* sp. strain NB4-1Y by Van Hamme et al. (2013) identified over 40 genes encoding proteins that have subsequently been annotated as acyl-CoA synthetase or acyl-CoA ligases.[14] Investigation into the transcriptomic response of *Gordonia* sp. strain NB4-1Y using 6:2 FTAB and 6:2 FTSA as sulfur sources found that the gene EMP12578.2, annotated as an acyl-CoA synthetase, had slightly higher expression in the presence of PFAS compared to magnesium sulfate controls.[24]

In this paper, we expressed and isolated acyl-CoA synthetase (designated ACS, UniProt: M7A1M8) encoded by EMP12578.2 and investigated the substrate scope and enzyme kinetics in the presence of various fluorinated and non-fluorinated carboxylates. We found that the NB4-1Y ACS can catalyze the formation of CoA adducts of short-chain fluorinated carboxylates, where the α-carbon is not fluorinated. This is the first time that these fluorinated CoA adducts have been identified and suggests that the metabolism of fluorinated carboxylates by *Gordonia* sp. strain NB4-1Y may proceed via the route proposed by Che et al.[25]

■ MATERIALS AND METHODS

Materials. 1:4 FTCA, 2:3 FTUA, 4,4,5,5,5-pentafluoro-pentanoic acid (2:3 FTCA), 3:3 FTCA, 5:3 FTCA. and 6:2 FTCA were purchased from SynQuest Laboratories (Alachua, FL, United States) with a purity of 95% or higher. *E. coli* BL21(DE3) was purchased from New England Biolabs (Ipswich, MA, United States). Protein purification supplies and columns were purchased from Cytiva (Marlborough, MA, United States). Bicinchoninic acid (BCA) protein assay was purchased from G-Biosciences (St Louis, MO, USA). All other chemicals were purchased from Sigma-Aldrich (Oakville, ON, Canada).

Production and Purification of ACS. A codon optimized synthetic gene encoding ACS, EMP 12578.2 from NB4-1Y, cloned into a pET28b(+) plasmid, was purchased from Genscript (Piscataway, NJ, United States). This fused an N-terminal His[6] tag to the recombinant protein. The gene-containing plasmid (designated pETACS) was transformed into *E. coli* BL21(DE3) for expression. Cells harboring pETACS were plated onto LB agar supplemented with kanamycin (50 μg/mL) and incubated at 37 °C for 16 h. A starter culture was prepared by inoculating 200 mL of LB medium, supplemented with kanamycin (50 μg/mL), and incubating for 16 h at 37 °C. Aliquots (25 mL) of the starter culture were added to 4 × 500 mL of terrific broth (TB) containing kanamycin (100 μg/mL) in 2 L flasks. Cultures were incubated at 30 °C with 200 rpm orbital shaking until the optical density at 600 nm was between 0.6 and 0.8. At this stage, isopropyl β-D-1-thiogalactopyranoside (IPTG) was added to a final concentration of 0.3 mM prior to incubating for 16 h at 25 °C at 200 rpm. Cells from 2 L of culture were harvested by centrifugation (6000 × *g*, 15 min, 4 °C) and cell pellets were stored at −80 °C.

Frozen cell pellets (~20 g) were resuspended on ice in 100 mL of 50 mM potassium phosphate (pH 7.5) containing phenylmethylsulfonyl fluoride (0.1 mM). Cell suspensions were sonicated for 15 min (15 s pulses at 1 min intervals) and then centrifuged at 40 000 × *g* for 50 min at 4 °C. Imidazole (20 mM) was added to the pooled supernatant, which was then applied to a 5 mL Ni-nitrilotriacetic acid column (NiNTA) equilibrated with 50 mM potassium phosphate, pH 7.5, and 0.02 M imidazole. The column was washed with 5 column volumes of equilibration buffer and 5 column volumes of 50 mM potassium phosphate (pH 7.5) with 40 mM imidazole. ACS was eluted with 50 mM potassium phosphate (pH 7.5) containing 0.3 M imidazole. ACS elution was detected by observing the absorbance at 280 nm. Fractions containing ACS were pooled and then dialyzed against 50 mM potassium phosphate and 0.05 M NaCl (pH 7.5). The

dialysate was then applied to a 50 mL Capto Q column equilibrated with 50 mM potassium phosphate with 0.05 M NaCl (pH 7.5). The protein was eluted with a linear gradient from 0.05 to 0.6 M NaCl. Fractions containing ACS were pooled and concentrated using a Centricon with a 10 kDa MW cutoff filter. SDS-polyacrylamide gel electrophoresis analysis confirmed protein identity with a MW of 60.8 kDa and protein concentration was determined via a BCA protein assay. The protein was frozen as a 20% glycerol stock and stored at −80 °C.

Product Analysis via Tandem Liquid Chromatography–Mass Spectrometry. To evaluate the substrate scope of ACS, a series of reactions were executed containing fluorinated and nonfluorinated carboxylates (Table 1). Reaction mixtures were in 50 mM potassium phosphate (pH 7.5) buffer containing 0.6 μM ACS, 4.5 mM ATP, 24 mM MgCl$_2$, 0.5 mM dithiothreitol (DTT), 0.5 mM CoA, and 50 mM carboxylate substrate. Reactions were incubated in an orbital shaker at 80 rpm for 24 h at 37 °C. After 24 h, ACS was filtered out using a 3 kDa cutoff centrifuge filter, and the filtrate was collected and placed into 2 mL glass injection vials containing a 50 μL glass insert for immediate liquid chromatography–mass spectrometry (LC–MS) analysis. Two controls were set up for each carboxylate substrate containing the same reaction mixture without either (1) ATP or (2) ACS. Standards containing 50 mM acetyl-CoA, propanoyl-CoA, hexanoyl-CoA or octanoyl-CoA were prepared in 50 mM potassium phosphate (pH 7.5) buffer. It was not possible to obtain standards for pentanoyl-CoA or any of the fluorinated CoA adducts as they were not commercially available.

Samples were analyzed on an Agilent 1200 series LC-HRMS system equipped with a C18 column coupled to an Agilent 6530 Accurate-Mass ESI quadrupole time-of-flight mass (Q-TOF) spectrometer following a method outlined by Keshet et al. (2022).[31] The mobile phases consisted of the following: (A) 100 mM ammonium acetate in water with 0.1% formic acid and (B) acetonitrile with 0.1% formic acid. The C18 column was maintained at 40 °C and the injection volume was 6.0 μL. At a flow rate of 0.3 mL/min, the LC gradient was as follows: 0 min, 1% B; 1.5 min, 1% B; 4.5 min, 15% B; 12.5 min, 25% B; 20 min, 95% B; 22 min, 95% B, followed by an additional 3 min postrun time to enable column equilibration to the initial solvent conditions. Positive electrospray (ESI) source parameters of the Q-TOF were set as follows: drying gas temperature, 250 °C; drying gas flow, 12 L/min; nebulizer pressure, 35 psi; sheath gas temperature, 350 °C; and sheath gas flow, 11 L/min. Extracted ion chromatograms (EICs) were obtained based upon theoretical m/z values ±0.1 with a mass error cutoff at ±10 ppm. Results were compared to control samples to eliminate background readings. Tandem mass spectrometry (MS/MS) with collision-induced dissociation (CID) spectra were obtained with a collision energy of 30 eV. Fragmentation spectra were compared to spectra predicated by CFM-ID 4.0 web server.[32]

Steady-State Kinetic Assays. AMP formation by ACS in the presence of ATP, CoA, and fluorinated and nonfluorinated carboxylates was monitored by a continuous coupled spectrophotometric assay utilized by Gallego-Jara et al. (2019).[28] This assay links AMP production to NADH oxidation monitored by ultraviolet–visible spectroscopy. Assay mixtures (1 mL total volume) were incubated at 25 °C in 50 mM potassium phosphate buffer (pH 7.5) containing

Table 1. Recorded m/z of CoA Adducts from LC–MS Spectra Detected Following 24 h of Incubation at 37 °C of Fluorinated and Nonfluorinated Carboxylates with CoA and ATP in the Presence of ACS[a]

carboxylate	structure	theoretical m/z of CoA adduct	experimental m/z of CoA adduct	retention time (min)
acetate		810.1330	810.1304	6.514
acetyl CoA standard[b]		810.1330	810.1403	5.984
fluoroacetate		828.1236	ND	-
difluoroacetate		846.1142	ND	-
trifluoroaceate		864.1047	ND	-
propionic acid		824.1487	824.1494	6.053
propionyl-CoA standard[b]		824.1487	824.1451	6.310
1:2 FTCA		878.1204	878.1165	7.037
pentafluoropropionic acid		914.1016	ND	-
pentanoic acid		852.1800	852.1823	10.589
1:4 FTCA		906.1517	906.1555	9.646
2:3 FTUA		904.1360	904.1355	8.210
2:3 FTCA		942.1328	942.1309	13.224
hexanoic acid		866.1956	866.1982	11.401
hexanoyl-CoA standard[b]		866.1956	866.1974	11.508
3:3 FTCA		992.1296	ND	-
perfluorohexanoic acid		1064.0920	ND	-
octanoic Acid		894.2270	ND	-
octanoyl-CoA standard[b]		894.2270	894.2278	16.506
5:3 FTCA		1092.1233	ND	-
6:2 FTCA		1128.1045	ND	-
perfluorooctanoic acid		1164.0856	ND	-

[a]This table also includes detected m/z of commercially available standards. ND = not detected. [b]Commercially available standards.

3.0 mM phosphoenolpyruvate (PEP), 10 units myokinase, 5 units pyruvate kinase, 7.5 units lactate dehydrogenase (LDH), 5 mM MgCl$_2$, 2.5 mM ATP, 1.5 mM CoA, 0.1 mM NADH, and 1 mM DTT. Reactions were initiated by the addition of 6

nM ACS and variable concentrations of a carboxylate (10 μM to 300 mM). Specific activity was determined by observing the oxidation of NADH at 340 nm using the extinction coefficient of NADH (6.22 mM^{-1} cm^{-1}). All reactions were performed in triplicate. Initial velocity data were fit to the Michaelis–Menten equation using RStudio to determine rate constant (k_{cat}), Michaelis constant (K_m), and catalytic efficiency (k_{cat}/K_m).

Sequence Alignment and Homology Modeling. The amino acid sequence of ACS was aligned with other members of the acyl-CoA synthetase family using Clustal Omega.[33] This includes the short-chain (<3 carbons) acyl-CoA synthetases (EC 6.2.1.1) from *E. coli* (UniProt: P27550), *Bacillus subtilis* (UnitProt: P39062), and *Burkholderia thailandensis* (UnitProt: Q2T3N9), a medium-chain (3−12 carbons) acyl-CoA synthetase (EC 6.2.1.2) from *Pseudomonas oleovorans* (UnitProt: Q00594), and the long-chain (>12 carbons) acyl-CoA synthetases (EC 6.2.1.3) from *E. coli* (UnitProt: P69451) and *Mycobacterium tuberculosis* (UnitProt: O53580).[34−39] The conserved ANL superfamily binding motifs (A1−A10) were identified when present. A predicted-homology model was constructed locally using AlphaFold v2.2.4 in the monomer mode with databases installed in July 2022 and db_preset set to full dbs.[40]

RESULTS

Substrate Scope of NB4-1Y ACS EMP12578.2. The ability of an NB4-1Y ACS (EMP12578.2) to catalyze the formation of CoA adducts of fluorinated and nonfluorinated carboxylates was assessed by LC−MS/MS analysis (Tables 2 and 3 and Figures S1 and S2).

With acetate (Table 1 and Figures S1A and S2A1), a compound with a retention time of 6.514 min and an m/z of 810.1304 was detected; this likely represents the formation of acetyl-CoA (theoretical m/z 810.1330) and is consistent with the spectra for the authentic acetyl-CoA standard (m/z

Table 2. Recorded m/z of Major Fragments of CoA Adducts Detected Via LC−MS/MS Following 24 h Incubation at 37 °C of Fluorinated and Nonfluorinated Carboxylates with CoA and ATP in the Presence of ACS[a]

carboxylate	predicted fragment m/z of CoA adducts[32]	experimental fragment m/z of CoA adducts
acetate	303.1373, 428.0367	303.1255, 428.0196
acetyl CoA standard[b]	303.1373, 428.0367	303.1453, 428.0471
propionic acid	317.1529, 428.0367	317.3185, 428.0550
propionyl-CoA standard[b]	317.1529, 428.0367	317.1556, 428.0358
1:2 FTCA	371.1247, 428.0367	371.1375, 428.0497
pentanoic acid	345.1843, 428.0367	345.1973, 428.0528
1:4 FTCA	399.1560, 428.0367	399.1574, 428.0388
2:3 FTUA	397.1403, 428.0367	397.1361, 428.0328
2:3 FTCA	435.1372, 428.0367	ND
hexanoic acid	359.1999, 428.0367	359.1963, 428.0320
hexanoyl-CoA standard[b]	359.1999, 428.0367	359.1924, 428.0273
octanoyl-CoA standard[b]	387.2312, 428.0367	387.2516, 428.0590

[a]This table also includes detected fragmentation m/z of commercially available standards and predicted fragment size determined by CFM-ID 4.0 web server. ND = not detected via MS/MS analysis. [b]Commercially available standards.

Table 3. Steady-State Kinetic Parameters for the Conversion to ATP to AMP in the Presence of ACS (6 nM), CoA, and Fluorinated and Nonfluorinated Carboxylate Substrates[a]

carboxylate	$k_{cat}/(s^{-1})$	K_m (mM)	k_{cat}/K_m (s^{-1} mM^{-1})
acetate	131 ± 5	78.3 ± 7.4	1.67 ± 0.22
fluoroacetate	ND		
difluoroacetate	ND		
trifluoroaceate	ND		
propionic acid	7.4 ± 0.2	1.7 ± 0.2	4.4 ± 0.5
1:2 FTCA	0.5 ± 0.1	NC	
pentafluoropropionic acid	ND		
pentanoic acid	18.6 ± 0.4	0.109 ± 0.011	170 ± 20
1:4 FTCA	1.99 ± 0.05	12.5 ± 0.7	0.16 ± 0.01
2:3 FTUA	0.19 ± 0.05	NC	
2:3 FTCA	0.09 ± 0.01	NC	
hexanoic acid	0.06 ± 0.01	NC	
3:3 FTCA	ND		
perfluorohexanoic acid	ND		
octanoic Acid	ND		
5:3 FTCA	ND		
6:2 FTCA	ND		
perfluorooctanoic acid	ND		

[a]Reactions were performed in 50 mM potassium phosphate (pH 7.5) at 25 °C. ND = no reaction detected. NC = K_m could not be accurately determined.

810.1403) (Figure S1I). The MS/MS spectra (Table 2 and Figure S2A2) displayed peaks at 303.1255 and 428.0196 consistent with both the standard (m/z 303.1453 and 428.0471) (Figure S2I2) and predicted fragmentation of acetyl-CoA (m/z 303.1373 and 428.0367).

In the reaction mixtures containing propanoic acid, pentanoic acid, and hexanoic acid, products were noted eluting at 6.053 min (m/z 824.1494), 10.589 (m/z 852.1823), and 11.401 (m/z 866.1982), respectively. These likely represent the production of propanoyl-CoA (theoretical m/z 824.1487), pentanoyl-CoA (theoretical m/z 852.1800), and hexanoyl-CoA (theoretical m/z 866.1956) (Table 1 and Figures S1B, S2B1, S1D, S2D1, S1H, and S2H1). The MS/MS spectra for the parent ion from each of these reaction mixtures included two major peaks (Table 2): propanoic acid product ions (m/z 317.3185 and 428.0550) (Figure S2B2), pentanoic acid product ions (m/z 345.1973 and 428.0528) (Figure S2D2), and hexanoic acid product ions (m/z 359.1963 and 428.0328) (Figure S2H2). Both the MS and MS/MS spectra were consistent with the authentic standards of propionyl-CoA (m/z 317.1556 and 428.0358) (Figure S2J2) and hexanoyl-CoA (m/z 359.1924 and 428.0273) (Figure S2K2) and with the fragments predicted using the CFM-ID 4.0 web server for propionyl-CoA (m/z 317.1529 and 428.0367) and hexanoyl-CoA (m/z 359.1999 and 428.0367). No authentic standard of pentanoyl-CoA was available for comparison; however, the fragments observed in the MS/MS were consistent with the predicted sizes (m/z 345.1843 and 428.0367). No reaction was detected with octanoic acid, as the filtered reaction mixture did not generate products consistent with the formation of octanoyl-CoA.

Under the chromatographic conditions used, and filtering chromatograms to within m/z ± 0.5, no CoA products were detected when ACS was reacted with fluoroacetate, difluoroacetate, or trifluoroacetate. For these and other fluorinated
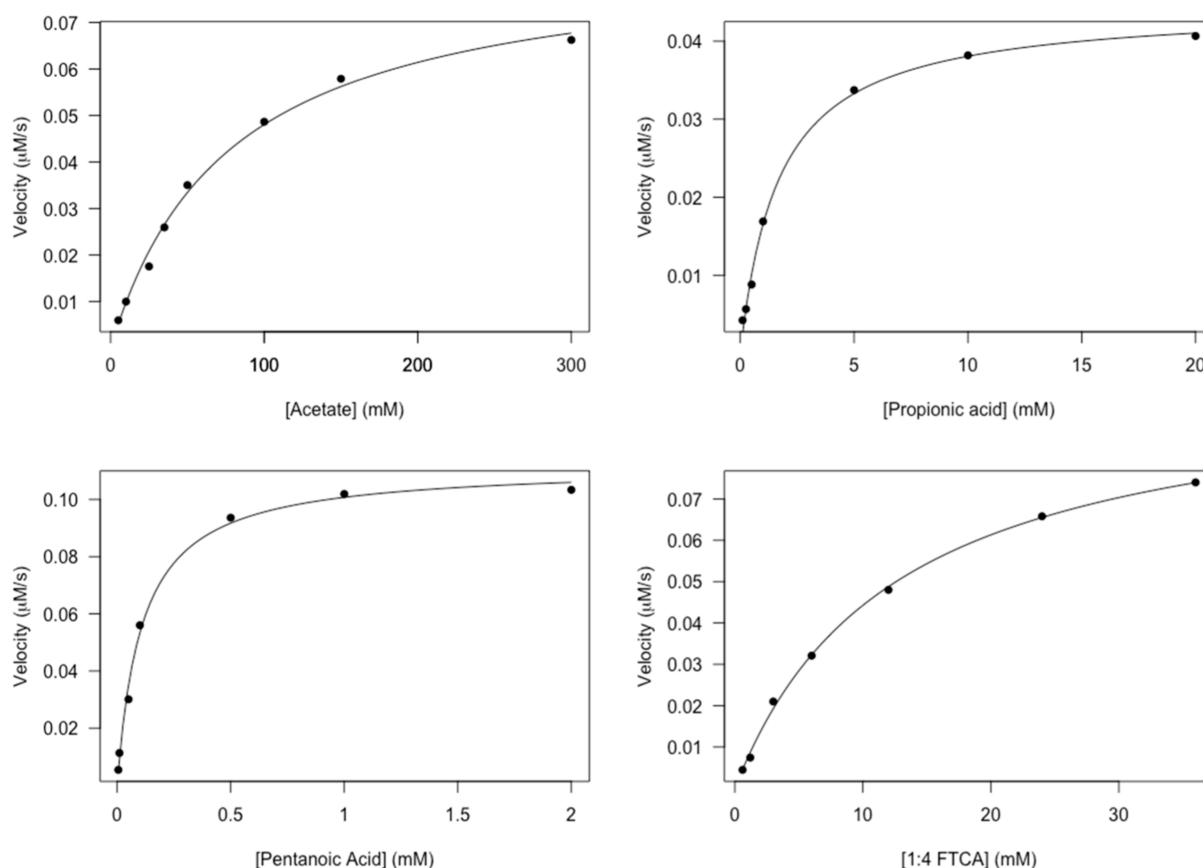
Figure 2. Michaelis−Menten plots showing the conversion of ATP to AMP by ACS (6 nM) with different carboxylate substrates. The initial velocity data were fit to the Michaelis−Menten equation, and kinetic parameters are presented in Table 3. The reactions were performed in 50 mM potassium phosphate (pH 7.5) at 25 °C.

compounds tested here, authentic standards of the corresponding CoA adducts were not available for analysis. Although these compounds have high solubility and cannot effectively be retained on a C18 column, their CoA adducts should be sufficiently retained. The very high initial concentration used in the reactions should also allow detection by the LC-HRMS system.

With 1:2 FTCA, a product was observed with an elution time of 7.037 min with m/z 878.1165, indicating the formation of 1:2 FTCA-CoA (theoretical m/z 878.1204) (Table 1 and Figures S1C and S2C1). Two major fragments were observed in the MS/MS spectra (m/z 371.1375 and 428.0497) (Figure S2C2) consistent with the predicted peaks for 1:2 FTCA-CoA (m/z 371.1247 and 428.0367). Reaction mixtures containing the fully fluorinated perfluoropropanoic acid did not generate any products that would suggest that a reaction had occurred.

Reaction mixtures containing 1:4 FTCA, 2:3 FTUA, and 2:3 FTCA generated compounds that eluted after 9.646 min (m/z 906.1555), 8.210 min (m/z 904.1355), and 13.224 min (m/z 942.1309), respectively (Table 1 and Figures S1E, S2E1, S1F, S2F1, S1G, and S2G1). These likely represent the formation of 1:4 FTCA-CoA (theoretical m/z 906.1517), 2:3 FTUA-CoA (theoretical m/z 904.1360), and 2:3 FTCA-CoA (theoretical m/z 942.1328). Two major fragments were observed in the MS/MS spectra (Table 2) for reactions with 1:4 FTCA (m/z 399.1574 and 428.0388) (Figure S2E2) and 2:3 FTUA (m/z 397.1361 and 428.0328) (Figure S2F2). These are consistent with the predicted values for 1:4 FTCA-CoA (m/z 399.1560 and 428.0367) and 2:3 FTUA-CoA (m/z 397.1403 and

428.0367). The concentration of the product from the reaction with 2:3 FTCA was too low to obtain a viable MS/MS spectrum.

The fluorinated hexanoic acid analogues: partially fluorinated 3:3 FTCA and fully fluorinated perfluorohexanoic acid, did not generate any eluates that would be consistent with the formation of CoA adducts. Similarly, fluorinated octanoic acid analogues: partially fluorinated 5:3 FTCA and 6:2 FTCA, and fully fluorinated perfluorooctanoic acid, also did not generate any eluates that would be consistent with the formation of CoA adducts.

Steady-State Kinetics of AMP Production. To determine whether there was selectivity toward certain substrates due to chain length or level of fluorination, the steady-state kinetic parameters of ACS associated with AMP production in the presence of various fluorinated and nonfluorinated carboxylate substrates were determined using a coupled kinetic assay. This enabled determination of the rate of conversion of ATP into AMP by observation of NADH oxidation at 340 nm. Where possible, initial rates were fit to the Michaelis−Menten equation to determine kinetic parameters, otherwise k_{cat} was estimated by the velocity at saturating substrate concentrations (Figure 2 and Table 3). Unsurprisingly, the 10 carboxylates tested (fluoroacetate, difluoroacetate, trifluoroacetate, pentafluoropropionic acid, 3:3 FTCA, perfluorohexanoic acid, octanoic acid, 5:3. FTCA, 6:2 FTCA, and perfluoroocatanoic acid) that did not show any observable production of CoA adducts via LC−MS, also did not have any detectable kinetic activity.

```
                                    A3 motif
                                  ━━━━━━━━━━━━━━
Gordonia sp. NB4-1Y              202 DDENTVITIN YTSGTTGKPKGV MYTHRGAYLNSFGE 237
Escherichia coli (EC:6.2.1.3)    203 LVPEDLAFLQ YTGGTTGVAKGA MLTHRNMLANLEQV 238
Escherichia coli (EC:6.2.1.1)    253 MNAEDPLFIL YTSGSTGKPKGV LHTTGGYLVYAALT 288
Mycobacterium tuberculosis       163 ERSADAIYLL YTGGTTGFPKGV MWRHEDIYRVLFGG 198
Bacillus subtilis                203 MDKKDGFLLH YTSGSTGTPKGV LHVHEAM-IQQYQT 237
Burkholderia thailandensis       259 VGAEHPLFIL YTSGSTGKPKGV QHSTAGYLLWVAQT 294
Pseudomonas oleovorans           174 VDENEASSLC YTSGTTGNPKGV LYSHRSTVLHSMTT 209

                                    A4 motif
                                  ━━━━━━━━━━━━━━
Gordonia sp. NB4-1Y              249 YLW TLPMFHC ---NGWC-----TPWAVTHASATHVC 276
Escherichia coli (EC:6.2.1.3)    254 -VT ALPLYHI FALTINC-----LLFIEL-GGQNLLI 282
Escherichia coli (EC:6.2.1.1)    300 ------IYWCTADVGWVTGHSYLLYGPLACGATTLM 329
Mycobacterium tuberculosis       225 RYP IPPMIHG ---ATQS-----ATWMALFSGQTTVL 252
Bacillus subtilis                249 ------IYWCTADPGWVTGTVYGIFAPWLNGATNVI 278
Burkholderia thailandensis       306 ------VFWCTADIGWVTGHSYITYGPLAVGATQVV 355
Pseudomonas oleovorans           223 ILP VVPMFHV NA---WG-----TPYSAAMVGAKLVL 250

                                    A5 motif
                                  ━━━━━━━━━━━━━━
Gordonia sp. NB4-1Y              345 V HVYGLTEV YGPYTICEYQDAWDDLDPAERAAKLSR 380
Escherichia coli (EC:6.2.1.3)    354 L EGYGLTEC APLVSVNPYDIDYHSG----------- 378
Escherichia coli (EC:6.2.1.1)    410 VDTWWQTET-GGFMITPLPG----------ATELKA 434
Mycobacterium tuberculosis       325 ----VITDSIGS-----SETGFGGTS---VVAAGQA 332
Bacillus subtilis                353 HDTWWMTET-GSQLICNYPC----------MDIKP 376
Burkholderia thailandensis       420 VDTWWQTET-GGHMITPLPG----------ATPTVP 444
Pseudomonas oleovorans           323 I HAWGMTEL SPFGTANTPLAHHVDLSPDEKLSLRKS 358

                      A7 motif              A8 motif
                  ━━━━━━━━━━━━━━━━       ━━━━━━━━━━━━━━
Gordonia sp. NB4-1Y              439 GWFHT GDLGVM-HPDGYIQL RDRAK DIIISGGEN IS 473
Escherichia coli (EC:6.2.1.3)    432 GWLHT GDIAVM-DEEGFLRI VDRKK DMILVSGFN VY 466
Escherichia coli (EC:6.2.1.1)    494 NMYFS GDGARR-DEDGYYWI TGRVD DVLNVSGHR LG 528
Mycobacterium tuberculosis       409 RYAIP GDYAQV-EEDGTVTM LGRGS VSINSGGEK VY 443
Bacillus subtilis                434 GWYVS GDSAYM-DEEGYFWF QGRVD DSINSGGEK VY 468
Burkholderia thailandensis       506 RLYLA GDGTVRDKETGYFTI MGRID DVLNVSGHR LG 541
Pseudomonas oleovorans           441 GWFST GDVATI-DSDGFMTI CDRAK DIIKSGGEW IS 455

                                    A10 motif
                              ━━━━━━━━━━━━━━━━━━━━━━━━
Gordonia sp. NB4-1Y              533 KVPRDIVFA DDLPRTSTGKVLKFELRKDAA EGSA-- 566
Escherichia coli (EC:6.2.1.3)    525 KVPKLVEFR DELPKSNVGKILRRELRDEAR GKVDNK 560
Escherichia coli (EC:6.2.1.1)    591 ATPDVLHWT DSLPKTRSGKIMRRILRKIAA GDTSNL 626
Mycobacterium tuberculosis       503 KVPRSLWFV DEVKRSPAGKPD-YRWAKEQT EARPAD 537
Bacillus subtilis                531 AAPREIEFK DKLPKTRSGKIMRRVLKAWEL N--LPA 564
Burkholderia thailandensis       607 AKPKDIRFG DNLPKTRSGKIMRRLLRSLAK GEAIT- 641
Pseudomonas oleovorans           505 QIPDAAIFV EELPRNGTGKILKNRLREKYG DILLRS 540
```

Figure 3. Sequence alignment of ACS with acyl-CoA synthetases from other prokaryotes aligned with Clustal Omega.[33] Short-chain acyl-CoA synthetases (EC 6.2.1.1) from *E. coli* (UniProt: P27550), *B. subtilis* (UnitProt: P39062) and *B. thailandensis* (UnitProt: Q2T3N9), a medium-chain acyl-CoA synthetase (EC 6.2.1.2) from *P. oleovorans* (UnitProt: Q00594), and the long-chain acyl-CoA synthetases (EC 6.2.1.3) from *E. coli* (UnitProt: P69451) and *M. tuberculosis* (UnitProt: O53580).[34−39]

With the nonfluorinated carboxylates, acetate was found to have the highest k_{cat} (131 ± 5 s^{-1}). There was a 7-fold decrease in activity with pentanoic acid (18.6 ± 0.4 s^{-1}) and a further decrease in activity for propanoic acid (7.4 ± 0.2 s^{-1}). The lowest recorded k_{cat} for the nonfluorinated carboxylates was found to be for hexanoic acid (0.06 ± 0.01 s^{-1}). Interestingly, the catalytic efficiency (k_{cat}/K_m) was found to be highest for the reaction with pentanoic acid (170 ± 20 s^{-1} mM^{-1}), and this parameter was found to decrease as the chain length decreased toward propanoic acid (4.4 ± 0.5 s^{-1} mM^{-1}) and acetate (1.67 ± 0.22 s^{-1} mM^{-1}). The activity for hexanoic acid was too low to enable an accurate determination of K_m.

For the fluorinated compounds, the activity was too low to allow for accurate determination of K_m. The highest k_{cat} recorded was with 1:4 FTCA (1.99 ± 0.05 s^{-1}) and, as with the nonfluorinated compounds, the five-carbon carboxylates resulted in higher activity than the three-carbon 1:2 FTCA (0.5 ± 0.1 s^{-1}). Finally, it was found that with increasing fluorination, there was a decrease in activity to 2:3 FTUA (0.19 ± 0.05 s^{-1}) and 2:3 FTCA (0.09 ± 0.01 s^{-1}). The catalytic efficiency for 1:4 FTCA (0.16 ± 0.01 s^{-1} mM^{-1}) was much lower than its nonfluorinated analogues.

In Silico Sequence Alignment and Homology Modeling to Determine Substrate Specificity. To gain further insights into the catalytic mechanism of ACS, sequence alignments with acyl-CoA synthetases from other organisms were performed with Clustal Omega. This analysis shows that the NB4-1Y ACS contains several conserved binding motifs from the SNL superfamily (Figure 3).[34−39] The A3, A7, A8, and A10 motifs show consensus with the other acyl-CoA synthases, while the A4 motif has no alignment with the short-chain acyl-CoA synthases (EC 6.2.1.1) but has moderate
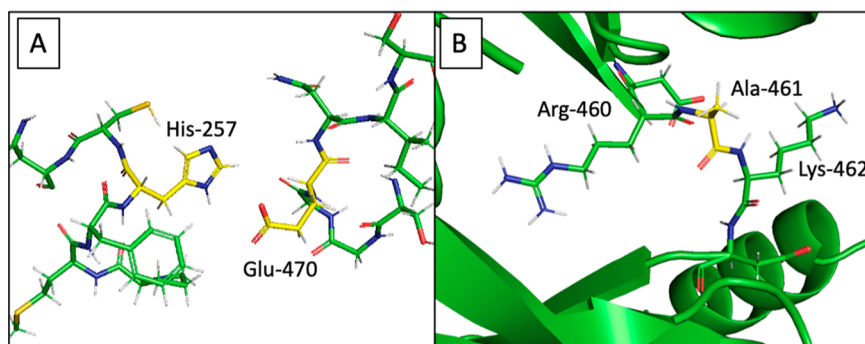
Figure 4. Homology model of the NB4-1Y ACS designed using AlphaFold2 showing: (A) Location of His-257 in the A4 motif and Glu-470 which is part of the A8 motif, and (B) part of the carboxylate binding loop, the presence of Ala-461.[27,40,41,42]

consensus with the medium- (EC 6.2.1.2) and long-chain acyl-CoA synthases (EC 6.2.1.3). Within this motif is residue His-257, which is present only in medium- and long-chain acyl-CoA synthases. Finally, the A5 motif shows moderate consensus with only the long-chain acyl-CoA synthetase from *E. coli* and the medium-chain acyl-CoA synthetase from *P. oleovorans*. Sequence alignment shows that the A4 motif contains His-257 and that the A8 motif contains Glu-470 (Figure 4A).

Sequence alignments show the presence of the aromatic His-257 in the NB4-1Y ACS; this residue forms part of the A4 motif and is generally conserved among long-chain and medium-chain acyl-CoA synthetases, while in short-chain acyl-CoA synthetases, this is often replaced by tryptophan.[27] This histidine residue forms a hydrogen bond with a glutamic acid residue in the A8 motif (Glu-470 in ACS), leading to rotation of the A8 motif into the active site (Figure 4A). This rotation allows the pantetheine group of CoA access to the bound carboxylate. In long-chain acyl-CoA synthetase from *E. coli*, there is a lysine residue prior to the A8 motif (Lys-454) that is hypothesized to be involved in controlling binding selectivity based upon the carboxylate chain length.[41] However, in medium-chain acyl-CoA synthetases, such as *Pseudomonas oleovorans* fatty acyl-CoA synthetase, this is replaced with alanine.[39] Sequence alignment and predictive homology modeling show that Ala-461 is present in this position in the amino acid sequence of ACS (Figure 4B).

DISCUSSION

Research into the removal of PFAS from the environment has become an important area of investigation due to increasing concerns about the health risks they pose to both humans and global ecosystems.[5,43,44] Studies with both pure microbial cultures and mixed microbial communities have revealed that bacteria and fungi are able to metabolize various PFAS, including 6:2 FTSA, 6:2 FTAB, and 6:2 fluorotelomer alcohol (FTOH), often leading to the production of fluorinated carboxylate intermediates such as 6:2 FTCA, 5:3 FTCA, and perfluoropentanoic acid.[16] However, the enzymatic pathways that facilitate the degradation of these have not been elucidated, although several metabolic routes have been proposed.[15,45] Short-chain PFAS are often produced as byproducts in the degradation of long-chain PFAS and the long-term effects of their presence in the environment have not been thoroughly investigated.[25] In addition, long-chain PFAS are difficult to handle in aqueous reaction mixtures due to low water solubilities, presenting challenges for in vitro enzymatic

analyses. However, short-chain PFAS dissolve in water more readily, and by investigating their properties, it may be possible to make predictions concerning the behavior of long-chain PFAS.

Che et al. (2021) proposed pathways for the degradation of the short-chain fluorinated carboxylates, 1:2 FTCA, 2:3 FTUA, and 1:4 FTCA, that begin with the formation of CoA adducts prior to diverging in downstream metabolic steps.[25] Specifically, they suggest that for the CoA adduct of 1:2 FTCA, there is a series of HF elimination reactions and subsequent hydrolysis to produce malonyl-CoA, which is then taken up by central metabolic pathways. 2:3 FTUA is proposed to undergo β-oxidation, hydration, HF-elimination, and hydrolysis to form monofluoromalonyl-CoA. Finally, following the addition of CoA, the reaction pathway of 1:4 FTCA is proposed to proceed via β-oxidation to form the CoA adduct of 1:2 FTCA. In their study, they identified intermediates associated with these pathways, including malonyl-CoA in the breakdown of 1:2 FTCA, 3-hydroxyl acid in the breakdown of 2:3 FTUA and 1:2 FTCA in the breakdown of 1:4 FTCA. It has also been proposed that long-chain PFAS, such as 8:2 FTUA, 6:2 FTUA and 6:2 FTCA, may also be metabolized via a β-oxidation pathway, which would also require the formation of a CoA adduct.[22] Bottos et al. (2020) discovered that a CoA transferase subunit A gene (RS05305) was expressed in *Gordonia* sp. strain NB4-1Y cultures grown in the presence of 6:2 FTAB, and an *N*-acetyltransferase gene (RS07500) was expressed in cultures grown in the presence of 6:2 FTAB and 6:2 FTSA.[24] This provides further indication that there may be CoA adducts formed by the bacterium during the breakdown of these compounds. However, until now, no CoA adducts have been detected for either long-chain or short-chain PFAS.

In this paper, we were able to confirm that reaction mixtures containing ATP, CoA, and either 1:2 FTCA, 1:4 FTCA, 2:3 FTUA, or 2:3 FTCA produced compounds with m/z consistent with the formation of 1:2 FTCA-CoA, 1:4 FTCA-CoA, 2:3 FTUA-CoA, and 2:3 FTCA-CoA, respectively. As such, the addition of CoA may indeed serve as the activation step of these short-chain fluorinated carboxylates for degradation pathways such as the ones proposed by Che et al.[25]

It was noted here that whenever the α-carbon of the carboxylate was partially or fully fluorinated, as in the case of fluoroacetate, difluoroacetate, trifluoroacetate, perfluoropropionic acid, perfluorohexanoic acid, and perfluorooctanoic acid, there was no reaction observed by either product detection or kinetic analysis. This may be due to fluorine

atoms on the α-carbon impeding the binding of the carboxylate to the active site or otherwise interfering with enzyme–substrate interactions. Due to the strength of the C–F bond, fluorinated substrate analogues can act as enzyme inhibitors, and that may be occurring when the α-carbon is fluorinated.[46,47] This is consistent with the findings by Che et al., where C–H bonds on the α-carbon were required for defluorination and short-chain perfluorinated acids were resistant to microbial degradation.[25]

Kinetic analysis of reactions catalyzed by the NB4-1Y ACS with nonfluorinated carboxylates showed that the highest catalytic efficiency was with pentanoic acid, and there was no observable reaction with octanoic acid. This suggests some specificity toward the substrate with the five-carbon chain. Analysis of the amino acid sequence of ACS revealed the conservation of multiple motifs (Figure 3), some of which may explain this specificity. The A3, A7, and A10 motifs are involved in the coordination of ATP binding, the A5 and A8 motifs are involved in the binding of the acyl-adenylate intermediate, and the A8 motif is involved in CoA binding.[26,48] The A4 motif tends to only be conserved among long-chain acyl-CoA synthetases and is involved in binding the carboxylate substrate.[48] The presence of His-257 and Glu-470 (Figure 4A) in NB4-1Y ACS is consistent with medium- and long-chain acyl-CoA synthases, while the presence of Ala-461 (Figure 4B) in place of a lysine suggests that ACS should act as a medium-chain acyl-CoA synthetase. This agrees with the kinetic data presented here, providing an explanation for the selectivity toward shorter-chain carboxylates over acetate or long-chain carboxylates.

Kinetic analysis of the reaction catalyzed by ACS with fluorinated carboxylates showed that there was a significant decrease in activity compared with the nonfluorinated analogues. There was a 90% decrease in k_{cat} with 1:4 FTCA compared to pentanoic acid and a 95% decrease in k_{cat} with 1:2 FTCA compared to propionic acid. In addition, as the pentanoic acid analogues became increasingly fluorinated, there was a significant decrease in the kinetic activity. This was expected, as we anticipated that the additional fluorine atoms would impede carboxylate binding and is consistent with the microbial sludge samples analyzed by Che et al. where there was 100% removal of 1:4 FTCA but only 30% removal of 2:3 FTUA.[25] There were no CoA adducts detected in the reaction with 3:3 FTCA; however, since a significant decrease in activity was observed with hexanoic acid; it is unsurprising that activity against the fluorinated analogue was undetectable under the conditions used.

This work indicates that *Gordonia* sp. strain NB4-1Y does contain enzymes capable of catalyzing a CoA activation step in the breakdown of short-chain fluorinated carboxylates and provides supporting evidence for the pathway proposed by Che et al.[25] We can hypothesize from this that other microorganisms capable of PFAS degradation may also contain enzymes that catalyze this activation step. This opens the possibility that there may be acyl-CoA synthetases specific to long-chain carboxylates that are involved in similar activation steps in the breakdown of long-chain fluorinated carboxylates. The next objective will be to identify enzymes that can catalyze the subsequent steps in the proposed mechanistic pathway: β-oxidation, hydrolysis, and defluorination. In addition, another investigative route will be to identify whether there are acyl-CoA synthetases capable of catalyzing reactions with long-chain fluorinated carboxylates.

■ ASSOCIATED CONTENT

Ⓢ Supporting Information

The Supporting Information is available free of charge at https://pubs.acs.org/doi/10.1021/acsomega.3c05147.

> LC–MS/MS spectra from reactions between carboxylates and CoA in the presence of ACS and of unreacted commercially available standards, EIC of filtrate based on predicted m/z values of reaction mixtures following 24 h incubation at 37 °C, and LC–MS/MS spectra of filtrate of reaction mixtures following 24 h incubation at 37 °C (PDF)

Accession Codes

UniProt: M7A1M8.

■ AUTHOR INFORMATION

Corresponding Author

Jonathan D. Van Hamme − *Department of Biological Sciences, Thompson Rivers University, Kamloops, BC V2C 0C8, Canada*; Phone: 250-377-6064; Email: jvanhamme@tru.ca

Authors

Robert G. Mothersole − *Department of Biological Sciences, Thompson Rivers University, Kamloops, BC V2C 0C8, Canada;* ⓞ orcid.org/0000-0001-7889-0988

Foster T. Wynne − *Department of Biological Sciences, Thompson Rivers University, Kamloops, BC V2C 0C8, Canada*

Gaia Rota − *Department of Biological Sciences, Thompson Rivers University, Kamloops, BC V2C 0C8, Canada*

Mina K. Mothersole − *Department of Biological Sciences, Thompson Rivers University, Kamloops, BC V2C 0C8, Canada*

Jinxia Liu − *Department of Civil Engineering, McGill University, Montreal, QC H3A 0C3, Canada;* ⓞ orcid.org/0000-0003-2505-9642

Complete contact information is available at:
https://pubs.acs.org/10.1021/acsomega.3c05147

■ ABBREVIATIONS

ACS, acyl-CoA synthetase; AFFF, aqueous film-forming foam; AMP, adenosine monophosphate; ANL, acyl-CoA synthetase, nonribosomal peptide synthetase adenylation domains, and luciferases; ATP, adenosine triphosphate; CID, collision-induced dissociation; CoA, coenzyme A; DTT, dithiothreitol; ESI, positive electrospray; FTAB, fluorotelomer sulfonami-doalkyl betaine; FTCA, saturated fluorotelomer carboxylate; FTSA, fluorotelomer sulfonate; FTUA, unsaturated fluoro-telomer carboxylate; LDH, lactate dehydrogenase; NAD,

nicotinamide adenine dinucleotide; NiNTA, Ni-nitrilotriacetic acid column; PEP, phosphoenolpyruvate; PFAS, perfluoroalkyl and polyfluoroalkyl substances; LC—MS/MS, tandem liquid chromatography—mass spectrometry

■ REFERENCES

(1) Borg, D.; Lund, B. O.; Lindquist, N. G.; Hakansson, H. Cumulative health risk assessment of 17 perfluoroalkylated and polyfluoroalkylated substances (PFASs) in the Swedish population. *Environ. Int.* **2013**, *59*, 112−123.

(2) Piekarski, D. J.; Diaz, K. R.; McNerney, M. W. Perfluoroalkyl chemicals in neurological health and disease: Human concerns and animal models. *Neurotoxicology* **2020**, *77*, 155−168.

(3) Fenton, S. E.; Ducatman, A.; Boobis, A.; DeWitt, J. C.; Lau, C.; Ng, C.; Smith, J. S.; Roberts, S. M. Per- and Polyfluoroalkyl Substance Toxicity and Human Health Review: Current State of Knowledge and Strategies for Informing Future Research. *Environ. Toxicol. Chem.* **2021**, *40* (3), 606−630.

(4) Dimzon, I. K.; Westerveld, J.; Gremmel, C.; Fromel, T.; Knepper, T. P.; de Voogt, P. Sampling and simultaneous determination of volatile per- and polyfluoroalkyl substances in wastewater treatment plant air and water. *Anal. Bioanal. Chem.* **2017**, *409* (5), 1395−1404.

(5) Hu, X. C.; Andrews, D. Q.; Lindstrom, A. B.; Bruton, T. A.; Schaider, L. A.; Grandjean, P.; Lohmann, R.; Carignan, C. C.; Blum, A.; Balan, S. A.; et al. Detection of Poly- and Perfluoroalkyl Substances (PFASs) in US Drinking Water Linked to Industrial Sites, Military Fire Training Areas, and Wastewater Treatment Plants. *Environ. Sci. Technol. Lett.* **2016**, *3* (10), 344−350.

(6) Sedlak, M. D.; Benskin, J. P.; Wong, A.; Grace, R.; Greig, D. J. Per-and polyfluoroalkyl substances (PFASs) in San Francisco Bay wildlife: Temporal trends, exposure pathways, and notable presence of precursor compounds. *Chemosphere* **2017**, *185*, 1217−1226.

(7) Ahrens, L.; Norstrom, K.; Viktor, T.; Cousins, A. P.; Josefsson, S. Stockholm Arlanda Airport as a source of per- and polyfluoroalkyl substances to water, sediment and fish. *Chemosphere* **2015**, *129*, 33−38.

(8) Domingo, J. L.; Nadal, M. Human exposure to per-and polyfluoroalkyl substances (PFAS) through drinking water: A review of the recent scientific literature. *Environ. Res.* **2019**, *177*, 108648.

(9) Andrews, D. Q.; Naidenko, O. V. Population-Wide Exposure to Per- and Polyfluoroalkyl Substances from Drinking Water in the United States. *Environ. Sci. Technol. Lett.* **2020**, *7* (12), 931−936.

(10) Grandjean, P.; Clapp, R. Perfluorinated Alkyl Substances: Emerging Insights Into Health Risks. *New Solut.* **2015**, *25* (2), 147−163.

(11) Barzen-Hanson, K. A.; Roberts, S. C.; Choyke, S.; Oetjen, K.; McAlees, A.; Riddell, N.; McCrindle, R.; Ferguson, P. L.; Higgins, C. P.; Field, J. A. Discovery of 40 Classes of Per- and Polyfluoroalkyl Substances in Historical Aqueous Film-Forming Foams (AFFFs) and AFFF-Impacted Groundwater. *Environ. Sci. Technol.* **2017**, *51* (4), 2047−2057.

(12) Backe, W. J.; Day, T. C.; Field, J. A. Zwitterionic, Cationic, and Anionic Fluorinated Chemicals in Aqueous Film Forming Foam Formulations and Groundwater from US Military Bases by Non-aqueous Large-Volume Injection HPLC-MS/MS. *Environ. Sci. Technol.* **2013**, *47* (10), 5226−5234.

(13) O'Carroll, D. M.; Jeffries, T. C.; Lee, M. J.; Le, S. T.; Yeung, A.; Wallace, S.; Battye, N.; Patch, D. J.; Manefield, M. J.; Weber, K. P. Developing a roadmap to determine per- and polyfluoroalkyl substances-microbial population interactions. *Sci. Total Environ.* **2020**, *712*, 135994.

(14) Van Hamme, J. D.; Bottos, E. M.; Bilbey, N. J.; Brewer, S. E. Genomic and proteomic characterization of *Gordonia* sp. NB4-1Y in relation to 6:2 fluorotelomer sulfonate biodegradation. *Microbiology* **2013**, *159*, 1618−1628.

(15) Shaw, D. M. J.; Munoz, G.; Bottos, E. M.; Duy, S. V.; Sauve, S.; Liu, J. X.; Van Hamme, J. D. Degradation and defluorination of 6:2 fluorotelomer sulfonamidoalkyl betaine and 6:2 fluorotelomer sulfonate by *Gordonia* sp. strain NB4-1Y under sulfur-limiting conditions. *Sci. Total Environ.* **2019**, *647*, 690−698.

(16) Zhang, Z. M.; Sarkar, D.; Biswas, J. K.; Datta, R. Biodegradation of per- and polyfluoroalkyl substances (PFAS): A review. *Bioresour. Technol.* **2022**, *344*, 126223.

(17) Li, R.; Munoz, G.; Liu, Y. N.; Sauve, S.; Ghoshal, S.; Liu, J. X. Transformation of novel polyfluoroalkyl substances (PFASs) as co-contaminants during biopile remediation of petroleum hydrocarbons. *J. Hazard. Mater.* **2019**, *362*, 140−147.

(18) Lenka, S. P.; Kah, M.; Padhye, L. P. A review of the occurrence, transformation, and removal of poly- and perfluoroalkyl substances (PFAS) in wastewater treatment plants. *Water Res.* **2021**, *199*, 117187.

(19) Houten, S. M.; Wanders, R. J. A. A general introduction to the biochemistry of mitochondrial fatty acid beta-oxidation. *J. Inherited Metab. Dis.* **2010**, *33* (5), 469−477.

(20) Dinglasan, M. J. A.; Ye, Y.; Edwards, E. A.; Mabury, S. A. Fluorotelomer alcohol biodegradation yields poly- and perfluorinated acids. *Environ. Sci. Technol.* **2004**, *38* (10), 2857−2864.

(21) Hagen, D. F.; Belisle, J.; Johnson, J. D.; Venkateswarlu, P. Characterization Of Fluorinated Metabolites By A Gas Chromatographic-Helium Microwave Plasma Detector - The Biotransformation Of 1h,1h,2h,2h-Perfluorodecanol To Perfluorooctanoate. *Anal. Biochem.* **1981**, *118* (2), 336−343.

(22) Martin, J. W.; Mabury, S. A.; O'Brien, P. J. Metabolic products and pathways of fluorotelomer alcohols in isolated rat hepatocytes. *Chem.-Biol. Interact.* **2005**, *155* (3), 165−180.

(23) Wang, N.; Szostek, B.; Folsom, P. W.; Sulecki, L. M.; Capka, V.; Buck, R. C.; Berti, W. R.; Gannon, J. T. Aerobic Biotransformation of ¹⁴C-Labeled 8-2 Telomer B Alcohol by Activated Sludge from a Domestic Sewage Treatment Plant. *Environ. Sci. Technol.* **2005**, *39* (2), 531−538.

(24) Bottos, E. M.; Al-shabib, E. Y.; Shaw, D. M. J.; McAmmond, B. M.; Sharma, A.; Suchan, D. M.; Cameron, A. D. S.; Van Hamme, J. D. Transcriptomic response of *Gordonia* sp. strain NB4-1Y when provided with 6:2 fluorotelomer sulfonamidoalkyl betaine or 6:2 fluorotelomer sulfonate as sole sulfur source. *Biodegradation* **2020**, *31* (4−6), 407−422.

(25) Che, S.; Jin, B. S.; Liu, Z. K.; Yu, Y. C.; Liu, J. Y.; Men, Y. J. Structure-Specific Aerobic Defluorination of Short-Chain Fluorinated Carboxylic Acids by Activated Sludge Communities. *Environ. Sci. Technol. Lett.* **2021**, *8* (8), 668−674.

(26) Morgan-Kiss, R. M.; Cronan, J. E. The *Escherichia coli fadK* (*ydiD*) gene encodes an anerobically regulated short chain acyl-CoA synthetase. *J. Biol. Chem.* **2004**, *279* (36), 37324−37333.

(27) Gulick, A. M. Conformational dynamics in the Acyl-CoA synthetases, adenylation domains of non-ribosomal peptide synthetases, and firefly luciferase. *ACS Chem. Biol.* **2009**, *4* (10), 811−827.

(28) Gallego-Jara, J.; Terol, G. L.; Écija Conesa, A.; Zambelli, B.; Cánovas Díaz, M.; de Diego Puente, T. Characterization of acetyl-CoA synthetase kinetics and ATP-binding. *Biochim. Biophys. Acta, Gen. Subj.* **2019**, *1863* (6), 1040−1049.

(29) Kim, Y. S.; Kang, S. W. Steady-state kinetics of malonyl-CoA synthetase from *Bradyrhizobium japonicum* and evidence for malonyl-AMP formation in the reaction. *Biochem. J.* **1994**, *297* (2), 327−333.

(30) Ingram-Smith, C.; Woods, B. I.; Smith, K. S. Characterization of the acyl substrate binding pocket of acetyl-CoA synthetase. *Biochemistry* **2006**, *45* (38), 11482−11490.

(31) Keshet, U.; Kind, T.; Lu, X. C.; Devi, S.; Fiehn, O. Acyl-CoA Identification in Mouse Liver Samples Using the In Silico CoA-Blast Tandem Mass Spectral Library. *Anal. Chem.* **2022**, *94* (6), 2732−2739.

(32) Wang, F.; Allen, D.; Tian, S. Y.; Oler, E.; Gautam, V.; Greiner, R.; Metz, T. O.; Wishart, D. S. CFM-ID 4.0-a web server for accurate MS-based metabolite identification. *Nucleic Acids Res.* **2022**, *50* (W1), W165−W174.

(33) Sievers, F.; Wilm, A.; Dineen, D.; Gibson, T. J.; Karplus, K.; Li, W.; Lopez, R.; McWilliam, H.; Remmert, M.; Söding, J.; et al. Fast,

scalable generation of high-quality protein multiple sequence alignments using Clustal Omega. *Mol. Syst. Biol.* **2011**, 7 (1), 539.

(34) Fulda, M.; Heinz, E.; Wolter, F. P. The *fadD* gene of *Escherichia coli* K12 is located close to rnd at 39.6 min of the chromosomal-map and is a new member of the AMP-binding protein family. *Mol. Gen. Genet.* **1994**, 242 (3), 241−249.

(35) BIattner, F. R.; Burland, V.; Plunkett, G.; Sofia, H.; Daniels, D. Analysis of the *Escherichia coli* genome. IV. DNA sequence of the region from 89.2 to 92.8 minutes. *Nucleic Acids Res.* **1993**, 21 (23), 5408−5417.

(36) Cole, S.; Brosch, R.; Parkhill, J.; Garnier, T.; Churcher, C.; Harris, D.; Gordon, S.; Eiglmeier, K.; Gas, S.; Barry, C. E.; et al. Deciphering the biology of *Mycobacterium tuberculosis* from the complete genome sequence. *Nature* **1998**, 396 (6707), 190.

(37) Grundy, F. J.; Waters, D. A.; Takova, T. Y.; Henkin, T. M. Identification of genes involved in utilization of acetate and acetoin in *Bacillus subtilis*. *Mol. Microbiol.* **1993**, 10 (2), 259−271.

(38) Kim, H. S.; Schell, M. A.; Yu, Y.; Ulrich, R. L.; Sarria, S. H.; Nierman, W. C.; DeShazer, D. Bacterial genome adaptation to niches: divergence of the potential virulence genes in three *Burkholderia* species of different survival strategies. *BMC Genomics* **2005**, 6 (1), 174−213.

(39) Beilen, J. B.; Eggink, G.; Enequist, H.; Bos, R.; Witholt, B. DNA-Sequence Determination And Functional-Characterization Of The Oct-Plasmid-Encoded *Alkjkl* Genes Of *Pseudomonas oleovorans*. *Mol. Microbiol.* **1992**, 6 (21), 3121−3136.

(40) Jumper, J.; Evans, R.; Pritzel, A.; Green, T.; Figurnov, M.; Ronneberger, O.; Tunyasuvunakool, K.; Bates, R.; Zidek, A.; Potapenko, A.; et al. Highly accurate protein structure prediction with AlphaFold. *Nature* **2021**, 596 (7873), 583−589.

(41) Black, P. N.; DiRusso, C. C.; Sherin, D.; MacColl, R.; Knudsen, J.; Weimar, J. D. Affinity labeling fatty acyl-CoA synthetase with 9-p-azidophenoxy nonanoic acid and the identification of the fatty acid-binding site. *J. Biol. Chem.* **2000**, 275 (49), 38547−38553.

(42) Varadi, M.; Anyango, S.; Deshpande, M.; Nair, S.; Natassia, C.; Yordanova, G.; Yuan, D.; Stroe, O.; Wood, G.; Laydon, A.; et al. AlphaFold Protein Structure Database: massively expanding the structural coverage of protein-sequence space with high-accuracy models. *Nucleic Acids Res.* **2022**, 50 (D1), D439−D444.

(43) Wang, Z. Y.; DeWitt, J. C.; Higgins, C. P.; Cousins, I. T. A Never-Ending Story of Per- and Polyfluoroalkyl Substances (PFASs)? *Environ. Sci. Technol.* **2017**, 51 (5), 2508−2518.

(44) Braun, J. M.; Chen, A. M.; Romano, M. E.; Calafat, A. M.; Webster, G. M.; Yolton, K.; Lanphear, B. P. Prenatal perfluoroalkyl substance exposure and child adiposity at 8 years of age: The HOME study. *Obesity* **2016**, 24 (1), 231−237.

(45) Kolanczyk, R. C.; Saley, M. R.; Serrano, J. A.; Daley, S. M.; Tapper, M. A. PFAS Biotransformation Pathways: A Species Comparison Study. *Toxics* **2023**, 11 (1), 74.

(46) Pongdee, R.; Liu, H. W. Elucidation of enzyme mechanisms using fluorinated substrate analogues. *Bioorg. Chem.* **2004**, 32 (5), 393−437.

(47) Abeles, R. H.; Alston, T. A. Enzyme-Inhibition By Fluoro Compounds. *J. Biol. Chem.* **1990**, 265 (28), 16705−16708.

(48) Chen, Y.; Sun, Y.; Song, H.; Guo, Z. Structural basis for the ATP-dependent configuration of adenylation active site in *Bacillus subtilis* o-succinylbenzoyl-CoA synthetase. *J. Biol. Chem.* **2015**, 290 (39), 23971−23983.